

Supporting Information

H-bond-induced luminescence enhancement in Pt₁Ag₃₀ nanocluster and its application in methanol detection

Silan Wang, Qinzhen Li, Sha Yang, Haizhu Yu, Jinsong Chai, and Manzhou Zhu**

Department of Chemistry and Centre for Atomic Engineering of Advanced Materials, Key Laboratory of Structure and Functional Regulation of Hybrid Materials of Ministry of Education, Institutes of Physical Science and Information Technology and Anhui Province Key, Laboratory of Chemistry for Inorganic/Organic Hybrid Functionalized Materials, Anhui University, Hefei, 230601, China

*E-mails of corresponding authors: chaijs@ahu.edu.cn; zmz@ahu.edu.cn

Notes: The authors declare no competing financial interest.

This Supporting Information includes:

Figures S1-S20

Tables S1-S2

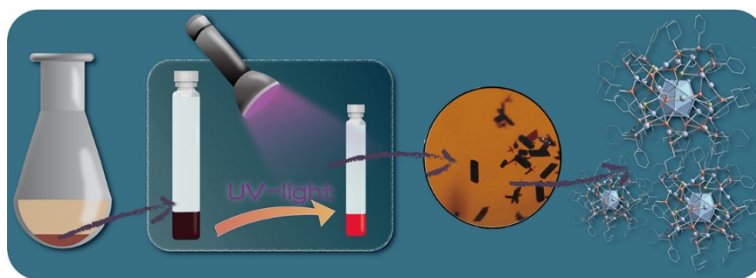


Figure S1. Schematic diagram of the crystallization process of $\text{Pt}_1\text{Ag}_{30}$.

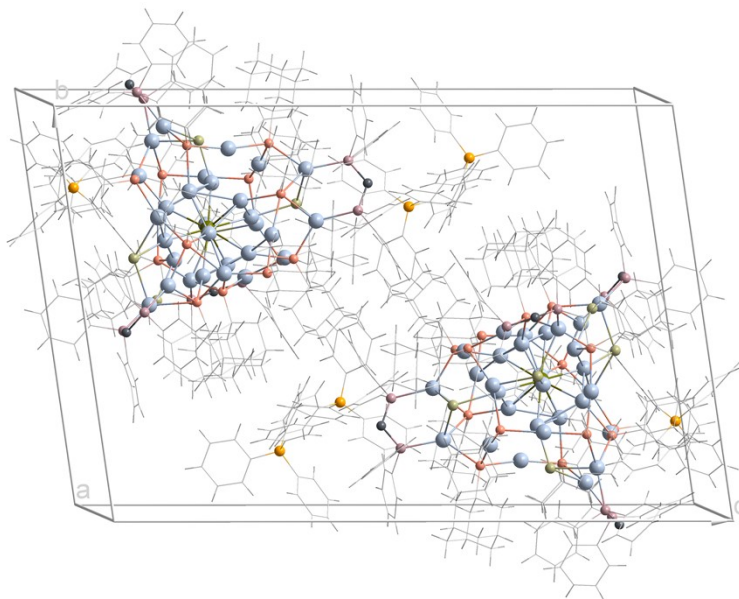


Figure S2. The unit cell of $[\text{Pt}_1\text{Ag}_{30}(\text{SAdm})_{14}(\text{Bdpm})_4\text{Cl}_5](\text{BPh}_4)_3$ (Color labels: blue = Ag; dark green = Pt; red = S; purple = P; yellow = B; dark grey = N).

To confirm the optimal excitation wavelength, the excitation spectra for the emission bands at 640 nm and 710 nm were measured, respectively (Figure S3 a). As shown in Figure S3 a, there are two excitation wavelengths located at 525 nm and 440 nm. Then, the 440 nm and 525 nm were employed as excitation wavelengths to measure the emission intensity of $\text{Pt}_1\text{Ag}_{30}$ dissolved in DCM, respectively. As shown in Figure S3 b, the intensity of photoluminescence is higher with the excitation wavelength at 440 nm than that at 525 nm. So, 440 nm was chosen as the optimal excitation wavelength for the photoluminescence test of the $\text{Pt}_1\text{Ag}_{30}$ nanocluster in this study.

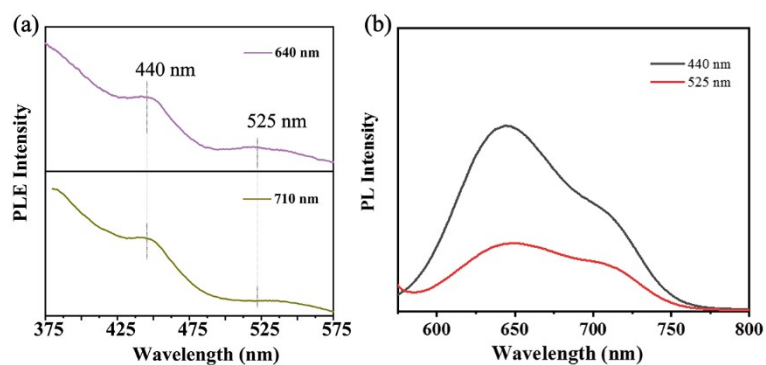


Figure S3. (a) The PL excitation spectra for the emission bands at 640 nm and 710 nm. (b) The PL emission spectra of Pt₁Ag₃₀ dissolved in DCM with the excitation wavelength of 440nm and 525 nm, respectively.

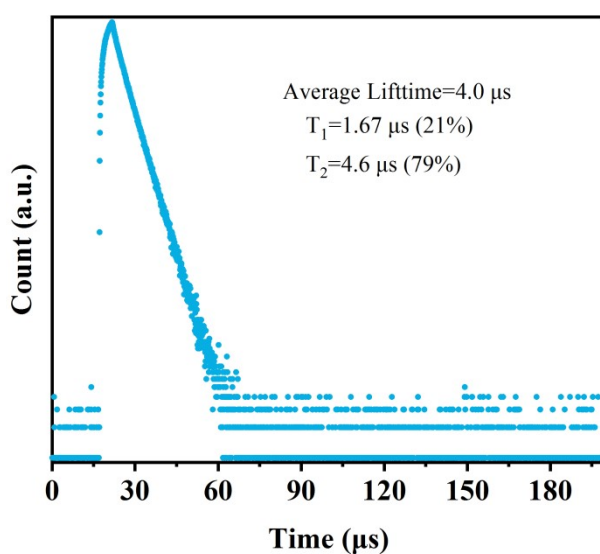


Figure S4. Time-correlated single-photon counting trajectories of Pt₁Ag₃₀ in ACN.

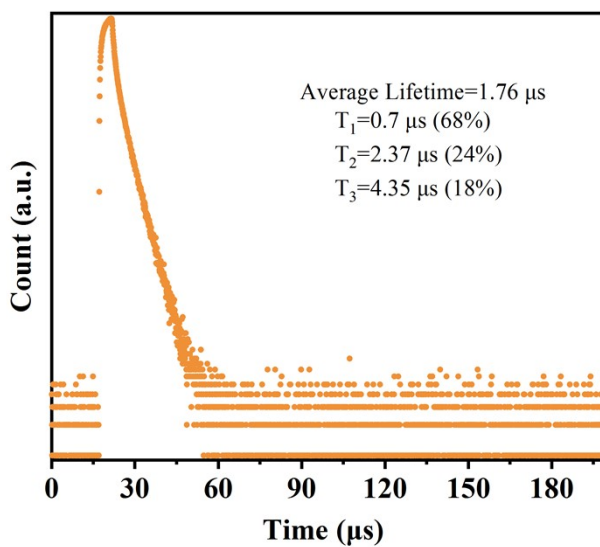


Figure S5. Time-correlated single-photon counting trajectories of Pt₁Ag₃₀ DMF.

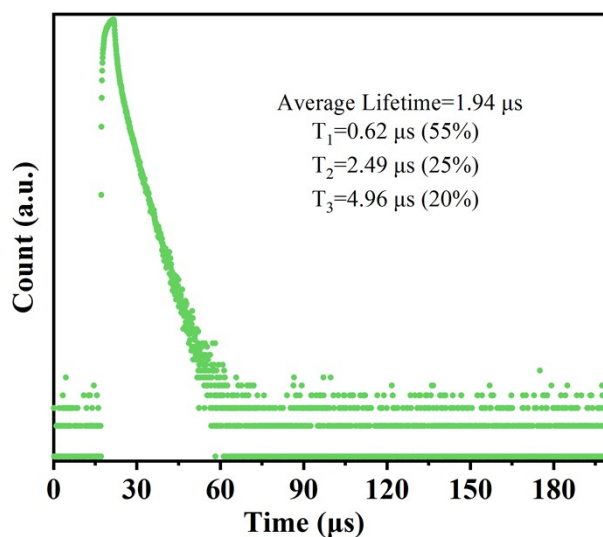


Figure S6. Time-correlated single-photon counting trajectories of $\text{Pt}_1\text{Ag}_{30}$ in acetone.

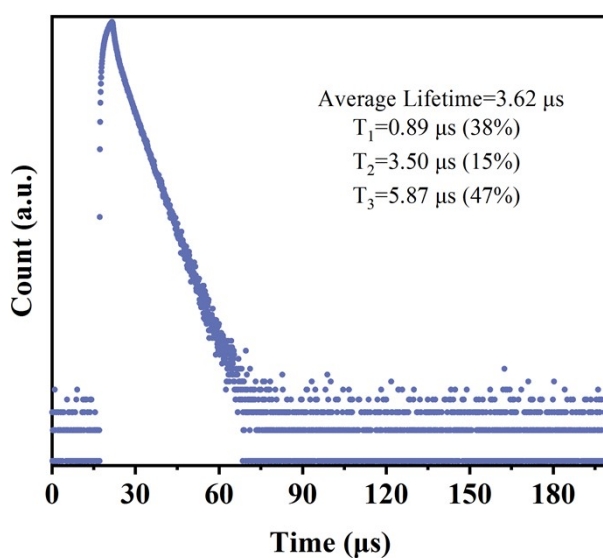


Figure S7. Time-correlated single-photon counting trajectories of $\text{Pt}_1\text{Ag}_{30}$ in TCM.

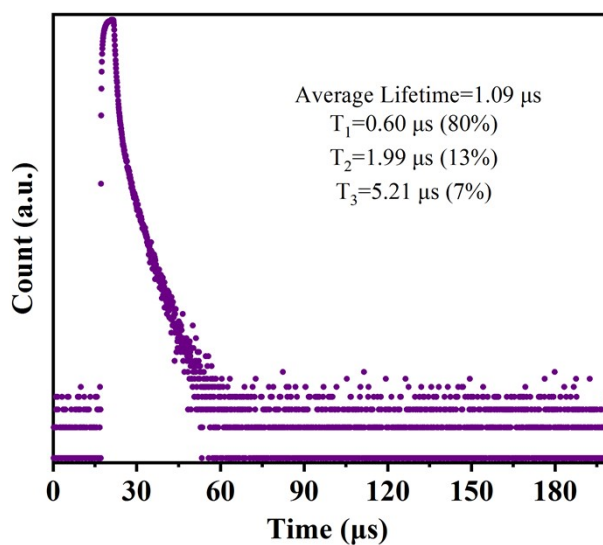


Figure S8. Time-correlated single-photon counting trajectories of $\text{Pt}_1\text{Ag}_{30}$ in THF.

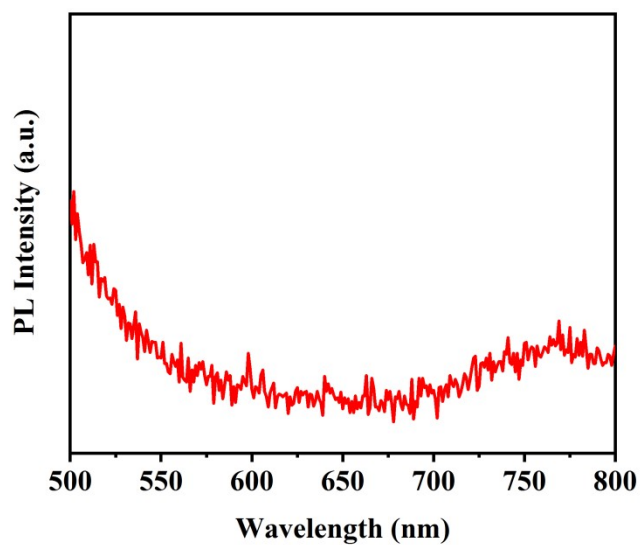


Figure S9. PL spectrum of $\text{Pt}_1\text{Ag}_{30}$ in a solid state.

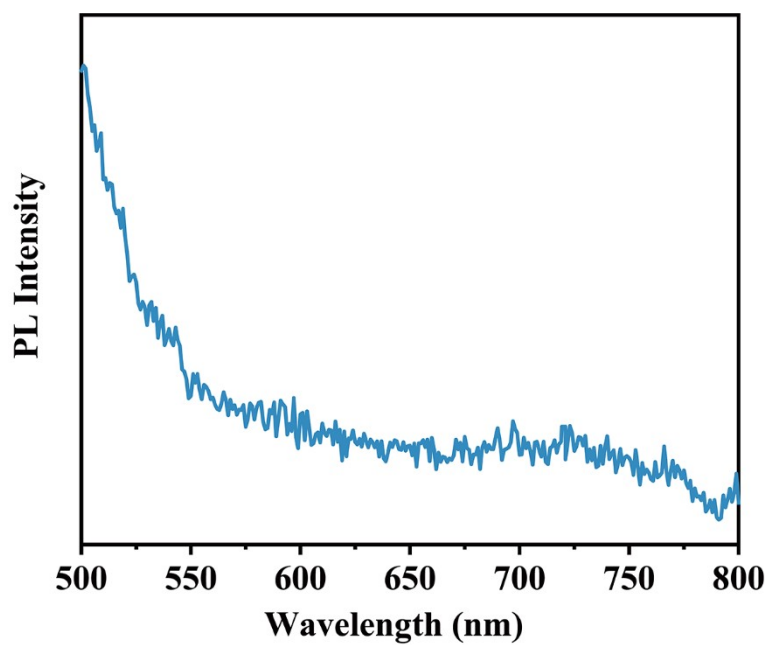


Figure S10. PL spectrum of $\text{Pt}_1\text{Ag}_{30}$ in single crystal state.

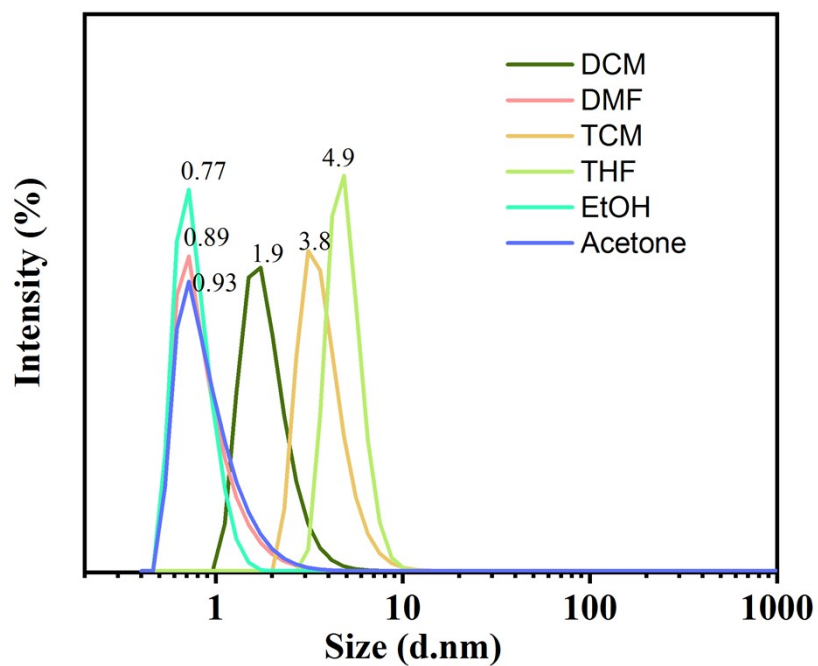


Figure S11. DLS measurement result of Pt_1Ag_{30} dissolved in DCM, DMF, TCM, THF, EtOH, and ACN.

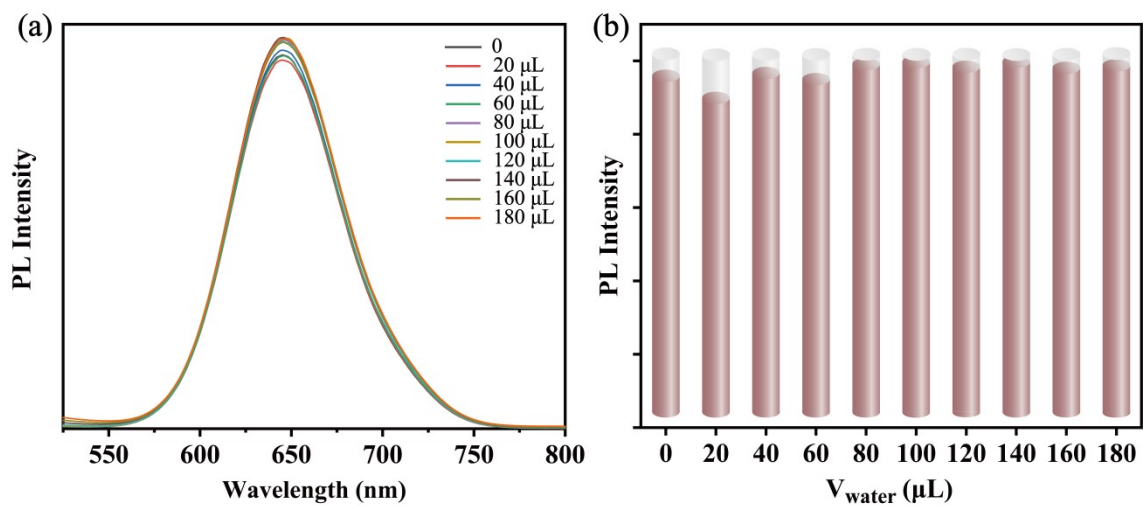


Figure S12. Fluorescence spectra tracing of adding H_2O to MeOH solution of Pt_1Ag_{30} .

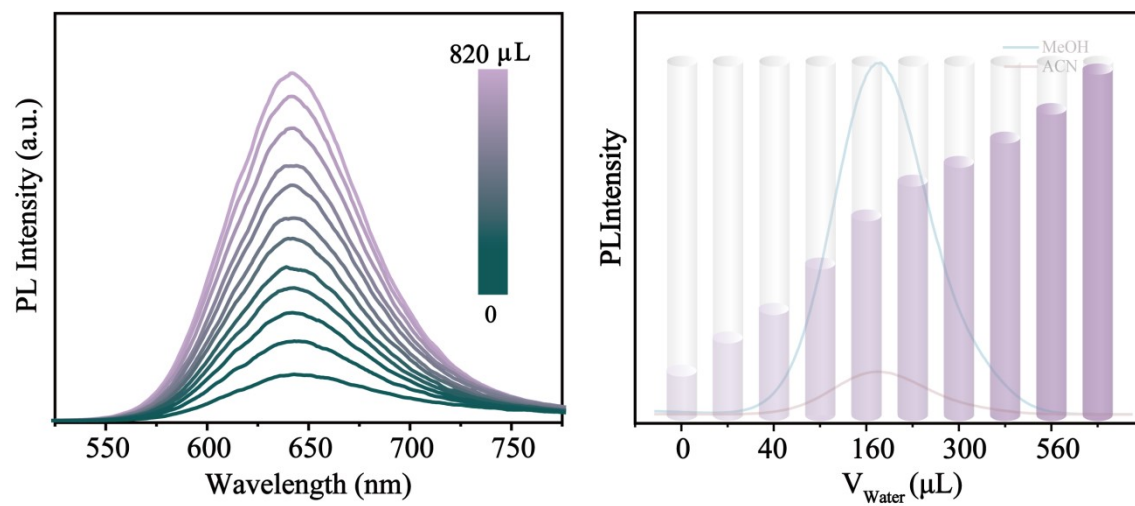


Figure S13. Fluorescence spectra tracing of adding H₂O to ACN solution of Pt₁Ag₃₀.

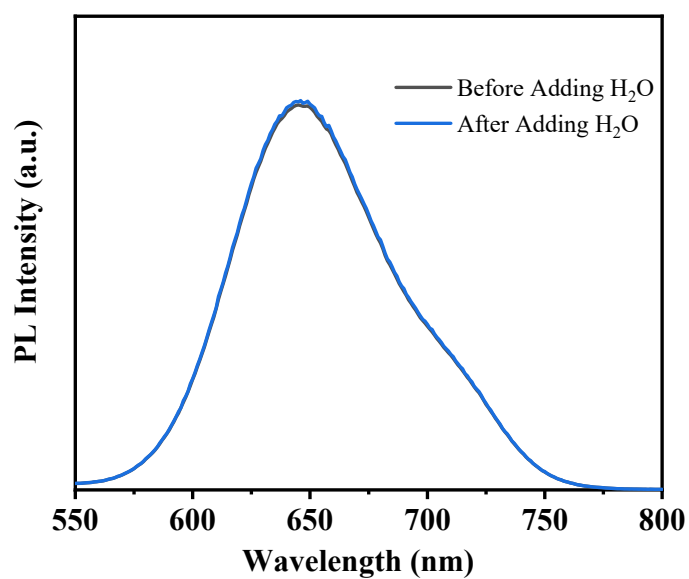


Figure S14. Fluorescence spectra tracing of adding H₂O to DCM solution of Pt₁Ag₃₀.

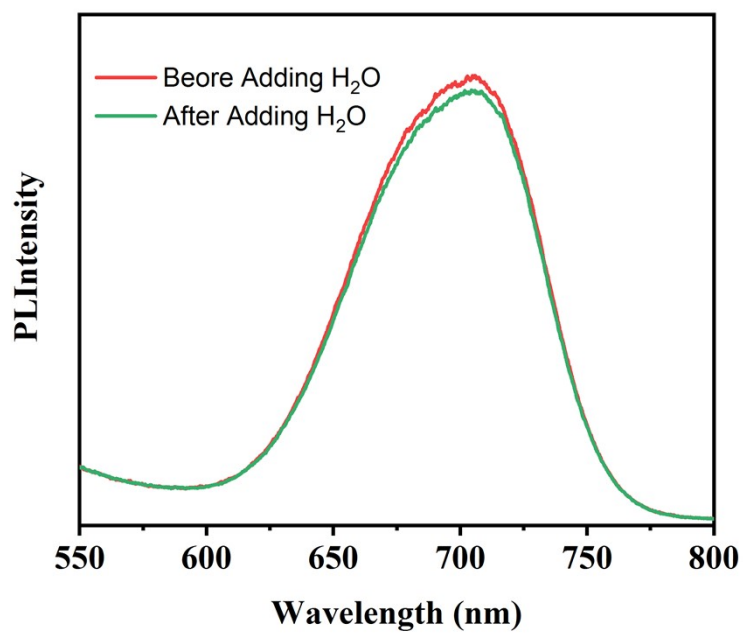


Figure S15. Fluorescence spectra tracing of adding H₂O to TCM solution of Pt₁Ag₃₀.

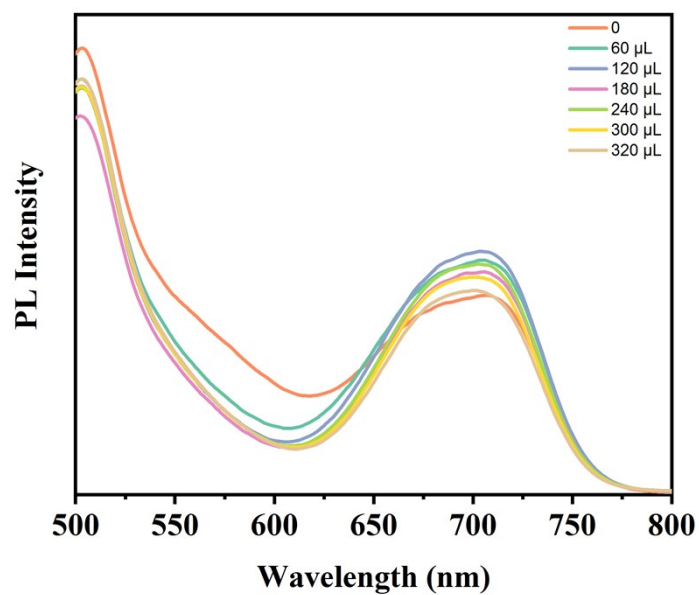


Figure S16. Fluorescence spectra tracing of adding H₂O to THF solution of Pt₁Ag₃₀.

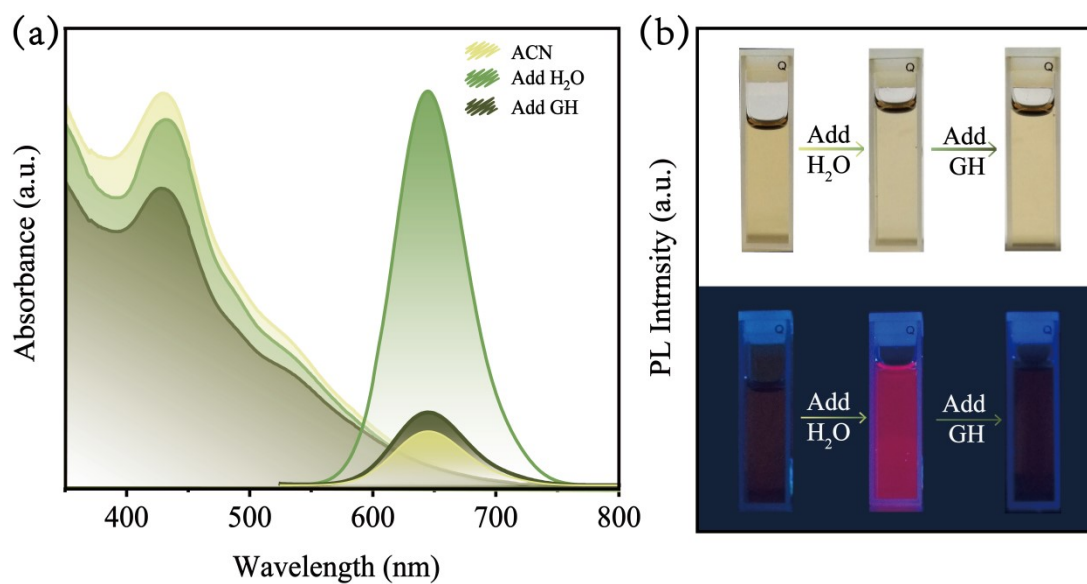


Figure S17. (a) Emissions and UV-Vis spectra of ACN solution of Pt_1Ag_{30} before adding H_2O , after adding H_2O , and after adding GH. (b) Photos of acetone solution under sunlight and UV-lamp in three states.

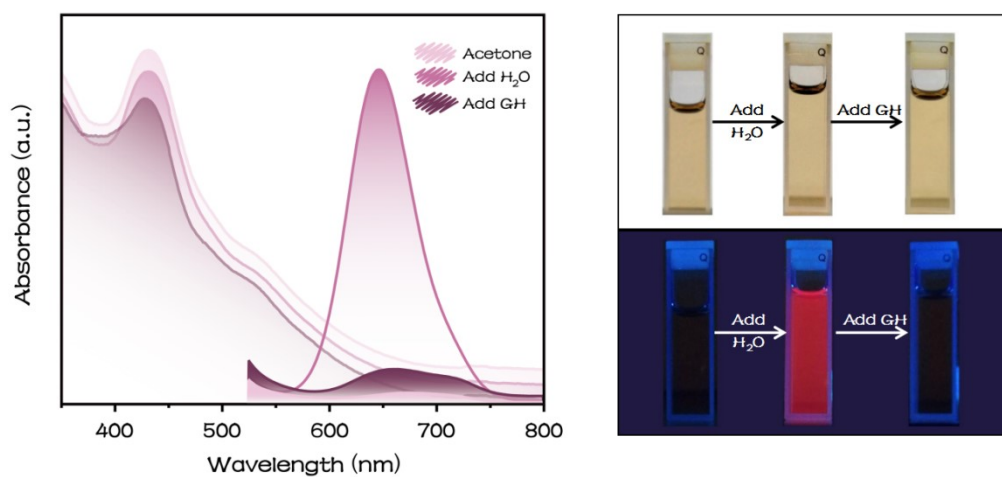


Figure S18. (a) Emissions and UV-Vis spectra of an acetone solution of Pt_1Ag_{30} before adding H_2O , after adding H_2O , and after adding GH. (b) Photos of acetone solution under sunlight and UV-lamp in three states.

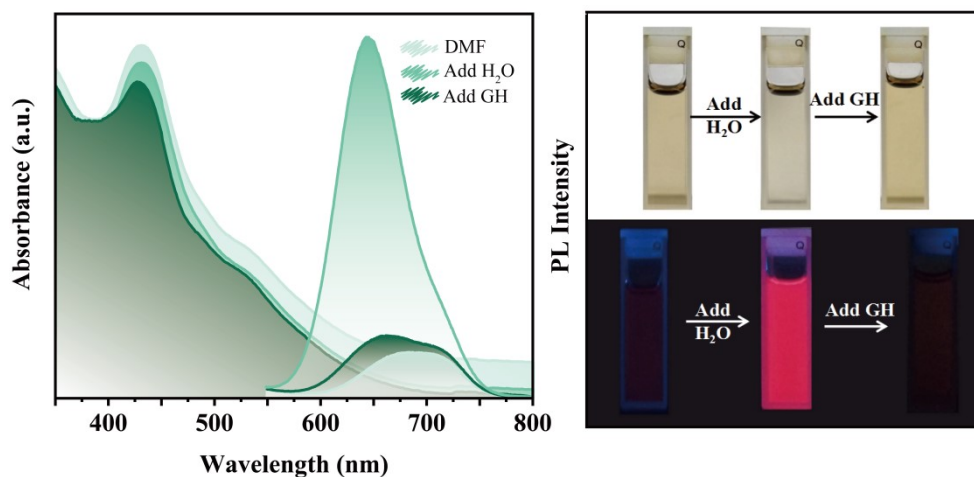


Figure S19. (a) Emissions and UV-Vis spectra of DMF solution of Pt₁Ag₃₀ before adding H₂O, after adding H₂O, and after adding GH. (b) Photos of DMF solution under sunlight and UV-lamp in three states.

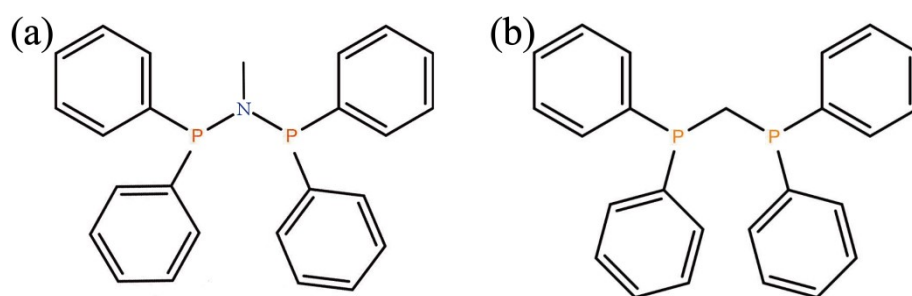


Figure S20. Structure diagram of BdpM (a) and DPPM (b).

Table S1. Fluorescence quantum yield of Pt₁Ag₃₀ in different solvents.

Solvent	QY
MeOH	15.36%
EtOH	2.18%
MeCN	3.08%
DCM	0.79%
TCM	0.31%
Acetone	0.26%
DMF	0.21%
THF	0.13%

Table S2 Crystal data and structure refinement for Pt₁Ag₃₀.

CCDC	2208493
Empirical formula	C ₃₃₃ H ₃₉₈ Ag ₃₀ B ₃ Cl ₃₃ N ₄ P ₈ PtS ₁₄
Formula weight	9786.97
Temperature/K	150
Crystal system	triclinic
Space group	P-1
a/Å	21.6934(3)
b/Å	23.8539(3)
c/Å	34.4020(5)
α/°	96.7550(10)
β/°	100.9060(10)
γ/°	100.2480(10)
Volume/Å ³	16989.5(4)
Z	2
ρ _{calc} /cm ³	1.913
μ/mm ⁻¹	18.211
F(000)	8908.0
Crystal size/mm ³	0.35 × 0.3 × 0.1
Radiation	CuKα (λ = 1.54186)
2θ range for data collection/	9.46 to 133.206
Index ranges	-16 ≤ h ≤ 25, -25 ≤ k ≤ 28, -40 ≤ l ≤ 40
Reflections collected	124446
Independent reflections	56983 [R _{int} = 0.0403, R _{sigma} = 0.0469]
Data/restraints/parameters	56983/1965/3521
Goodness-of-fit on F ²	1.025
Final R indexes [I >= 2σ (I)]	R ₁ = 0.0613, wR ₂ = 0.1672
Final R indexes [all data]	R ₁ = 0.0777, wR ₂ = 0.1779
Largest diff. peak/hole / e Å ⁻³	3.20/-1.42
